

# Diacylglycerol kinase $\zeta$ is a negative regulator of GPVI-mediated platelet activation

Alyssa J. Moroi,<sup>1</sup> Nicole M. Zwifelhofer,<sup>1</sup> Matthew J. Riese,<sup>1-3</sup> Debra K. Newman,<sup>1,3,4</sup> and Peter J. Newman<sup>1,4,5</sup>

<sup>1</sup>Blood Research Institute, Versiti, Milwaukee, WI; <sup>2</sup>Department of Hematology-Oncology, <sup>3</sup>Department of Microbiology and Immunology, <sup>4</sup>Department of Pharmacology and Toxicology, and <sup>5</sup>Department of Cell Biology, Neurobiology, and Anatomy, Medical College of Wisconsin, Milwaukee, WI

## Key Points

- DGK $\zeta$  is a novel negative regulator of GPVI-mediated platelet activation.
- Loss of DGK $\zeta$  upregulates surface expression of GPVI in platelets and megakaryocytes.

Diacylglycerol kinases (DGKs) are a family of enzymes that convert diacylglycerol (DAG) into phosphatidic acid (PA). The  $\zeta$  isoform of DGK (DGK $\zeta$ ) has been reported to inhibit T-cell responsiveness by downregulating intracellular levels of DAG. However, its role in platelet function remains undefined. In this study, we show that DGK $\zeta$  was expressed at significant levels in both platelets and megakaryocytes and that DGK $\zeta$ -knockout (DGK $\zeta$ -KO) mouse platelets were hyperreactive to glycoprotein VI (GPVI) agonists, as assessed by aggregation, spreading, granule secretion, and activation of relevant signal transduction molecules. In contrast, they were less responsive to thrombin. Platelets from DGK $\zeta$ -KO mice accumulated faster on collagen-coated microfluidic surfaces under conditions of arterial shear and stopped blood flow faster after ferric chloride-induced carotid artery injury. Other measures of hemostasis, as measured by tail bleeding time and rotational thromboelastometry analysis, were normal. Interestingly, DGK $\zeta$  deficiency led to increased GPVI expression on the platelet and megakaryocyte surfaces without affecting the expression of other platelet surface receptors. These results implicate DGK $\zeta$  as a novel negative regulator of GPVI-mediated platelet activation that plays an important role in regulating thrombus formation in vivo.

## Introduction

Platelets circulate in blood vessels, serving as cellular sentries for physical or chemical vascular injury. Should the endothelial cell lining become damaged, platelets interact via their glycoprotein Ib (GPIb)-V-IX receptor complex with collagen-bound von Willebrand factor,<sup>1</sup> tethering them to the subendothelial lining, and cell surface GPVI can interact with collagen. GPVI/collagen interactions initiate signaling events that lead to the generation of second messengers, such as Ca<sup>2+</sup> and diacylglycerol (DAG).<sup>2</sup> DAG is generated from phosphatidyl inositol 4,5 biphosphate by the  $\beta$  isoform of phospholipase C (PLC $\beta$ ) downstream of G protein-coupled receptors and by the  $\gamma$ 2 isoform of PLC (PLC $\gamma$ 2) downstream of (hem) immunoreceptor tyrosine-based activation motif receptors.<sup>3</sup> DAG is also formed through dephosphorylation of phosphatidic acid (PA) by PA phosphatase.<sup>4</sup> DAG binds to and activates multiple isoforms of the serine/threonine protein kinase PKC, which in turn phosphorylates a wide range of substrates, ultimately leading to integrin activation, granule secretion, and other platelet activation events that stabilize the hemostatic thrombus, sometimes referred to as the platelet plug.<sup>3,5</sup> Therefore, regulation of intracellular DAG level is an important early event in the platelet activation process.

Diacylglycerol kinases (DGKs) are a family of enzymes thought to suppress cellular activation by reducing the level of DAG via conversion of DAG to PA.<sup>6-8</sup> The DGK family consists of 10 isozymes ( $\alpha$ ,  $\beta$ ,  $\gamma$ ,  $\delta$ ,  $\eta$ ,  $\kappa$ ,  $\epsilon$ ,  $\zeta$ ,  $\iota$ , and  $\theta$ ) that are divided into 5 classes based on structure. DGK proteins have been isolated from human platelets,<sup>9</sup> and reverse transcription polymerase chain reaction (RT-PCR) analysis showed that human platelets express most of the isozymes, with the exception of DGK $\beta$  and  $\theta$ .<sup>10</sup> Type I

DGKs (DGK $\alpha$ ,  $\beta$ , and  $\gamma$ ) have been the most studied, largely because of the availability of inhibitors, and have been reported to have functional roles in human platelets. For example, treating human platelets with the type I DGK inhibitor R59949 resulted in enhanced platelet aggregation in response to vasopressin, collagen, and U46619.<sup>11,12</sup> Although R59949 had no effect on thrombin-mediated platelet aggregation, it reduced calcium mobilization after thrombin stimulation, suggesting that type I DGKs differentially regulate GPVI- vs thrombin-mediated platelet activation.<sup>10</sup> R59022, another type 1 DGK inhibitor, has variously been shown to suppress<sup>13</sup> or potentiate<sup>14</sup> thrombin-induced platelet aggregation. However, discrepant findings from these studies have resulted in confusion regarding the actual role of the various DGK isozymes in platelet activation.

DGK $\zeta$  is a type IV DGK that is widely expressed in different cell types and tissues.<sup>15-19</sup> T cells are known to express high levels of DGK $\zeta$ ,<sup>7,20</sup> and DGK $\zeta$ -knockout (DGK $\zeta$ -KO) mice exhibit a mild increase in the number of CD8<sup>+</sup> T cells, together with elevated intracellular levels of DAG and enhanced Ras-ERK signaling after T-cell receptor engagement.<sup>19,21,22</sup> DGK $\zeta$ -KO T cells also show increased upregulation of activation markers, proliferation, and enhanced responses to pathogens. Interestingly, RNA-sequencing analysis revealed that DGK $\zeta$  is the most abundant DGK isozyme in mouse platelets and the third most abundant in human platelets.<sup>23</sup> However, whether DGK $\zeta$  is expressed in platelets at the protein level and whether it plays any role in thrombosis and hemostasis are unknown. Therefore, the purpose of the present study was to examine these issues and determine the functional consequences of DGK $\zeta$  deficiency.

## Methods

### Mice

DGK $\zeta$ -KO mice (C57BL/6J background) have previously been described.<sup>19</sup> Wild-type (WT) C57BL/6J mice were obtained from littermate controls or purchased from The Jackson Laboratory (Bar Harbor, ME). Mice were maintained in the Biological Resource Center at the Medical College of Wisconsin. All animal protocols were approved by the Medical College of Wisconsin Institutional Animal Care and Use Committee. All studies were performed using mice of either sex between the ages of 10 and 20 weeks.

### Blood parameter analysis

Blood was drawn from the inferior vena cava, and blood cell counts were measured using the scil Vet ABC Hematology Analyzer (scil Corporation, Gurnee, IL).

### Platelet flow cytometry

Platelet surface receptor expression was measured in whole blood after staining with the indicated fluorescein isothiocyanate-conjugated antibodies using the BD Accuri C6 Plus (BD Biosciences). Data were analyzed using FlowJo software (Tree Star, Ashland, OR). The extent of agonist-induced platelet activation was assessed by staining agonist-stimulated washed platelets with activation-specific markers (fluorescein isothiocyanate-conjugated anti-P-selectin or phycoerythrin-conjugated Jon/A).

### Mouse platelet isolation

Washed platelets were prepared as previously described<sup>24</sup> with modification in Tyrode's buffer (137 mM of sodium chloride, 2.5 mM of potassium chloride, 0.36 mM of sodium dihydrogen phosphate

dihydrate, 13.8 mM of sodium bicarbonate, 20 mM of *N*-2-hydroxyethylpiperazine-*N'*-2-ethanesulfonic acid, and 0.1% glucose). Washed platelets were resuspended in Tyrode's buffer to an appropriate concentration for the experiments.

### Western blotting

Washed platelets were stimulated with collagen-related peptide (CRP; 1  $\mu$ g/mL) at 37°C with stirring for the indicated times, and reactions were terminated by adding an equal volume of ice-cold 2 $\times$  lysis buffer (300 mM of sodium chloride, 20 mM of tris[hydroxymethyl]aminomethane, 2 mM of EGTA, 2 mM of EDTA, and 2% NP40 [pH, 7.5]). The samples were diluted with an equal volume of 2 $\times$  sample buffer (4% sodium dodecyl sulfate, 10% 2-mercaptoethanol, 20% glycerol, and 50 mM of tris[hydroxymethyl]aminomethane [pH, 6.8]), separated by sodium dodecyl sulfate polyacrylamide gel electrophoresis, and transferred to a poly(vinylidene difluoride) membrane. Western blotting was performed with the indicated antibodies. Bands were quantitated by densitometry using IMAGE J software (National Institutes of Health, Bethesda, MD).

### Platelet aggregation and secretion

Aggregation was monitored by light transmission with a Born Lumi-Aggregometer (Chrono-log Corporation). Platelet adenosine triphosphate release was measured using luciferin/luciferase reagent (Chrono-lume; Chrono-log Corporation).

### Platelet spreading

Eight-chamber glass tissue culture slides (Corning, Corning, NY) were coated with 1% bovine serum albumin (BSA), 50  $\mu$ g/mL of collagen, 50  $\mu$ g/mL of CRP, or 30  $\mu$ g/mL of fibrinogen at 4°C overnight. Wells were blocked with 1% BSA. Washed platelets (200  $\mu$ L; 2  $\times$  10<sup>7</sup>/mL) in Tyrode's buffer supplemented with 1 mM of calcium chloride were allowed to spread for the indicated times at 37°C. Adherent platelets were fixed with 5% neutral buffered formalin and permeabilized with 0.1% Triton-X100. The fixed platelets were stained with phalloidin-TRITC (10  $\mu$ g/mL). Images were taken with an inverted microscope (Nikon, Melville, NY). Platelet spreading area was analyzed using IMAGE J software, and results are reported as the mean area of spread platelets ( $\mu$ m<sup>2</sup> per platelet).

### Tail bleeding assay

Blood loss was measured in 10- to 15-week-old WT and DGK $\zeta$ -KO mice after excision of a tail at a distance of 1 mm from the tip. The time to cessation of bleeding was recorded.

### ROTEM analysis

Whole blood was collected from the vena cava and diluted at a ratio of 1:9 (volume/volume) with 3.8% sodium citrate. Thrombocytopenic blood was prepared as previously described.<sup>25</sup> Hemostasis in mouse whole blood at the described platelet count was measured by rotational thromboelastometry (ROTEM) using the ROTEM delta (ROTEM, Durham, NC).

### FeCl<sub>3</sub>-induced thrombus formation

Mice were anesthetized, and the right carotid arteries were detached from surrounding tissues. Vascular injury was induced by applying a filter paper saturated with 10% ferric chloride (FeCl<sub>3</sub>) to the top of the vessel for 3 minutes. A microvascular flow probe attached to a transit-time perivascular flowmeter (Transonic, Ithaca,

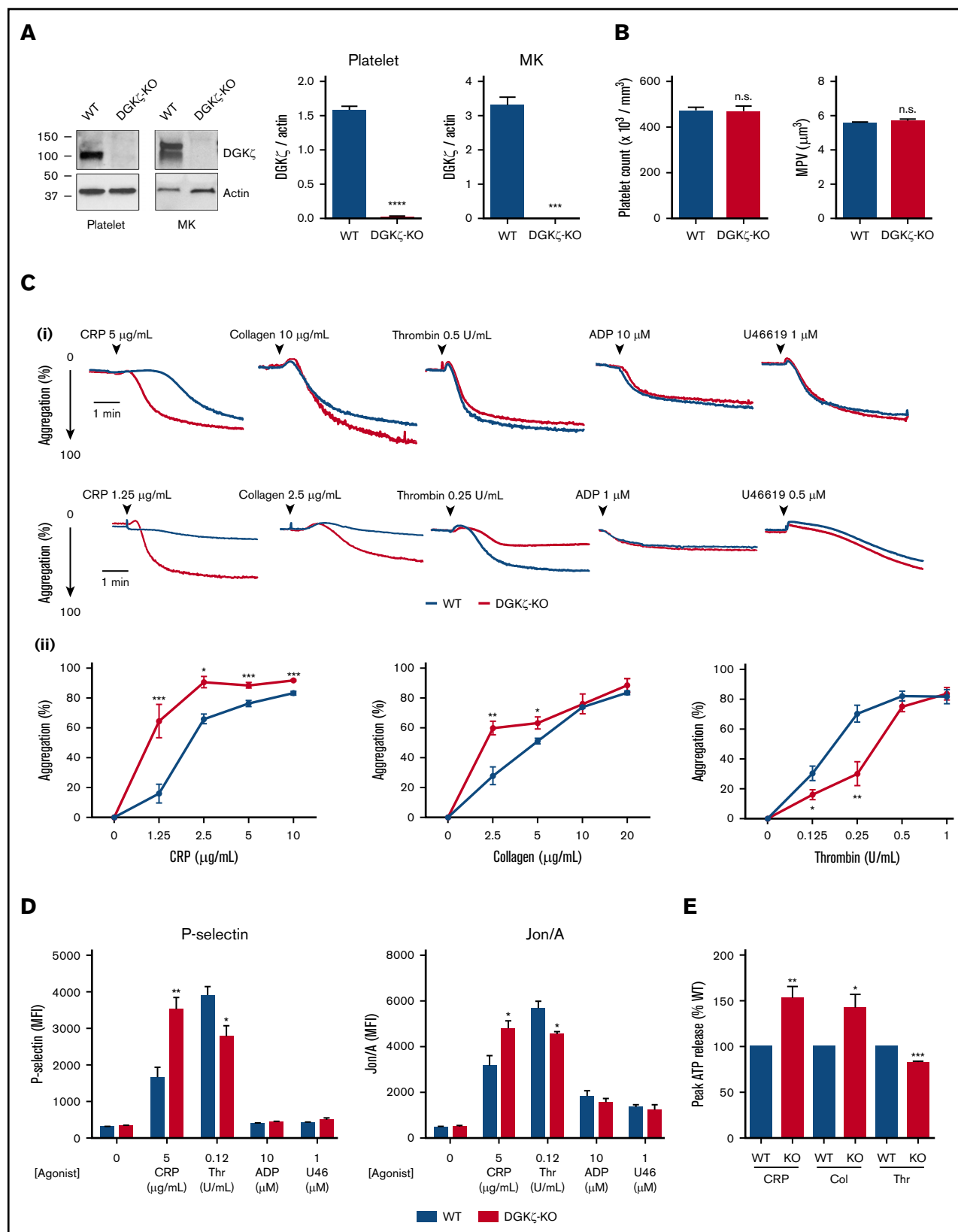


**Figure 1. DGK $\zeta$  negatively regulates GPVI-mediated platelet activation but enhances thrombin (Thr)-mediated platelet activation.** (A) Whole lysates of washed platelets and megakaryocytes (MKs) from WT and DGK $\zeta$ -KO mice were analyzed by western blotting for DGK $\zeta$  and actin. The blot shown on the left is representative of 3 to 4 independent experiments. Quantification of band densities (right) is reported as the mean  $\pm$  SEM ( $n = 3-4$ ). (B) Platelet counts (left) and mean platelet volumes

**Table 1. Blood parameters of WT and DGK $\zeta$ -KO mice (n = 20)**

Blood parameter	Mean $\pm$ SEM				
	Platelet count, 10 <sup>6</sup> /mL	Platelet volume, $\mu\text{m}^3$	WBC count, 10 <sup>6</sup> /mL	RBC count, 10 <sup>9</sup> /mL	Hematocrit, %
WT	469.7 $\pm$ 16.2	5.5 $\pm$ 0.1	2.9 $\pm$ 0.3	7.0 $\pm$ 0.2	33.4 $\pm$ 0.8
DGK $\zeta$ -KO	466.8 $\pm$ 24.2	5.7 $\pm$ 0.1	2.7 $\pm$ 0.2	6.9 $\pm$ 0.2	33.9 $\pm$ 0.9

RBC, red blood cell; WBC, white blood cell.

NY) was positioned on the carotid artery to monitor blood flow. Blood flow was recorded from immediately after removing the filter paper until 3 minutes after full occlusion. The time to first occlusion was defined by blood flow of  $<0.05$  mL per minute.

### In vitro platelet adhesion and thrombus formation in microfluidic chambers

Whole blood was collected and anticoagulated with heparin/PPACK and labeled with mepacrine (Calbiochem). Thrombus formation on collagen was performed as previously described<sup>24</sup> on collagen (50  $\mu\text{g}/\text{mL}$ ) at an arterial shear rate of 1500  $\text{s}^{-1}$ . Images of platelet adhesion and thrombus formation were acquired by epifluorescence microscopy at a rate of 1 frame per second. Platelet accumulation was analyzed using IMAGE J software, and results are reported as the mean area covered by platelet aggregates (%). For 3-dimensional image analysis, microchannels were washed with phosphate-buffered saline at the end of flow analysis and fixed, permeabilized, and stained with phalloidin-TRITC. Z stack images were taken using step changes of 1.16  $\mu\text{m}$  with an FV1000 Olympus laser scanning confocal microscope (Olympus, Tokyo, Japan) and analyzed using Slidebook 6 software (Intelligent Imaging Innovations, Denver, CO). Results were reported as thrombus volume and height.

### Mouse megakaryocyte isolation and culture

Bone marrow cells were collected and resuspended in ammonium-chloride-potassium buffer (0.15 M of ammonium chloride, 1 mM of potassium bicarbonate, and 0.1 mM of disodium EDTA [pH, 7.3]) to remove red cells. Cells expressing Gr-1, CD11b, B220, and CD16/32 were depleted using magnetic Dynabeads. The remaining cells were cultured in complete Stempro medium (Gibco, Grand Island, NY) supplemented with 20 ng/mL of murine stem cell factor (SCF) for 2 days and then further cultured in the presence of 20 ng/mL of murine SCF and 50 ng/mL of murine thrombopoietin (TPO). After 5 days of culture in SCF/TPO-supplemented medium, mature megakaryocytes were enriched by BSA gradient.

### Quantitative RT-PCR

RNA was isolated from mature megakaryocytes with the RNeasy Mini Plus Kit (Qiagen, Germantown, MD). RNA was then converted

to complementary DNA using the SuperScript III Kit (Invitrogen). RT-PCR was performed in triplicate using the PrimeTime Std qPCR Assay (IDT, San Jose, CA) with Brilliant II SYBR Green QPCR Master Mix (Agilent Technologies, Santa Clara, CA) in an ABI 7500 (Applied Biosystems, Foster City, CA). Transcripts for hypoxanthine-guanine phosphoribosyltransferase, integrin  $\alpha\text{IIb}$ , GPIb $\alpha$ , GPVI, integrin  $\alpha 2$ , FcR $\gamma$  chain, and DGK $\zeta$  were analyzed. Relative gene expression levels were calculated using the comparative  $C_T$  method, using hypoxanthine-guanine phosphoribosyltransferase for normalization.

### Statistics

All experiments were performed  $>3$  times, with data shown as the mean  $\pm$  standard error of the mean (SEM). Statistical analysis was performed using unpaired Student *t* test using Prism 6.0 software (GraphPad, San Diego, CA).

## Results

### DGK $\zeta$ -KO platelets are hyperreactive to GPVI agonists

Splice variants of DGK $\zeta$  having different *N*-termini have been identified in T cells and macrophages.<sup>19,26</sup> As shown in Figure 1A, only the short isoform was present in WT mouse platelets, and this was absent in DGK $\zeta$ -KO mouse platelets. However, WT mouse megakaryocytes expressed both the long and short isoforms, both of which were absent in DGK $\zeta$ -KO megakaryocytes (Figure 1A). Expression of other DGK isozyme expressions ( $\alpha$ ,  $\gamma$ , and  $\epsilon$ ) were comparable between WT and DGK $\zeta$ -KO platelets (supplemental Figure 1A). DGK $\zeta$ -KO mice had normal platelet counts and mean platelet volumes, indicating that they have normal thrombopoiesis (Figure 1B). No differences in other blood parameters, such as white or red blood cell count, were observed (Table 1).

To determine the consequences of DGK $\zeta$  deficiency for platelet function, the responsiveness of DGK $\zeta$ -KO vs WT platelets after stimulation with platelet agonists was assessed. As shown in Figure 1C, platelet aggregation in response to collagen or the GPVI-specific agonist CRP was potentiated in DGK $\zeta$ -KO relative to WT platelets. In contrast, the response to a submaximal concentration of

**Figure 1. (continued)** (MPVs; right) observed in WT and DGK $\zeta$ -KO mice. Values represent means  $\pm$  SEM (n = 20). (Ci) Aggregation of washed platelets from WT and DGK $\zeta$ -KO mice was measured by lumiaggregometry in response to high (top) and low (bottom) doses of CRP, collagen (Col), Thr, adenosine 5'-diphosphate (ADP), and U46619. Each aggregation tracing is representative of 3 to 5 independent experiments. (ii) Dose-response curve of maximal platelet aggregation after CRP, Col, and Thr stimulation. Values represent the mean  $\pm$  SEM of maximal platelet aggregation observed in 3 to 4 independent experiments. (D) P-selectin exposure (left) and Jon/A binding as a reporter of activation of integrin  $\alpha\text{IIb}\beta 3$  (right) were measured by flow cytometry in washed platelets after 20 minutes of stimulation with CRP, Thr, ADP, and U46619 (U46) at the indicated concentrations. Values represent the mean  $\pm$  SEM of mean fluorescence intensity (MFI) observed in 5 independent experiments. (E) Quantification of peak adenosine triphosphate (ATP) released from platelets stimulated with CRP (2.5  $\mu\text{g}/\text{mL}$ ), Col (5  $\mu\text{g}/\text{mL}$ ), and Thr (0.5 U/mL) relative to WT. ATP release was measured by lumiaggregometry. Values represent the mean  $\pm$  SEM observed in 3 to 5 independent experiments. Statistical analysis was performed by the unpaired Student *t* test. \**P* < .05, \*\**P* < .01, \*\*\**P* < .001, \*\*\*\**P* < .0001 of DGK $\zeta$ -KO as compared with WT. n.s., not significant.

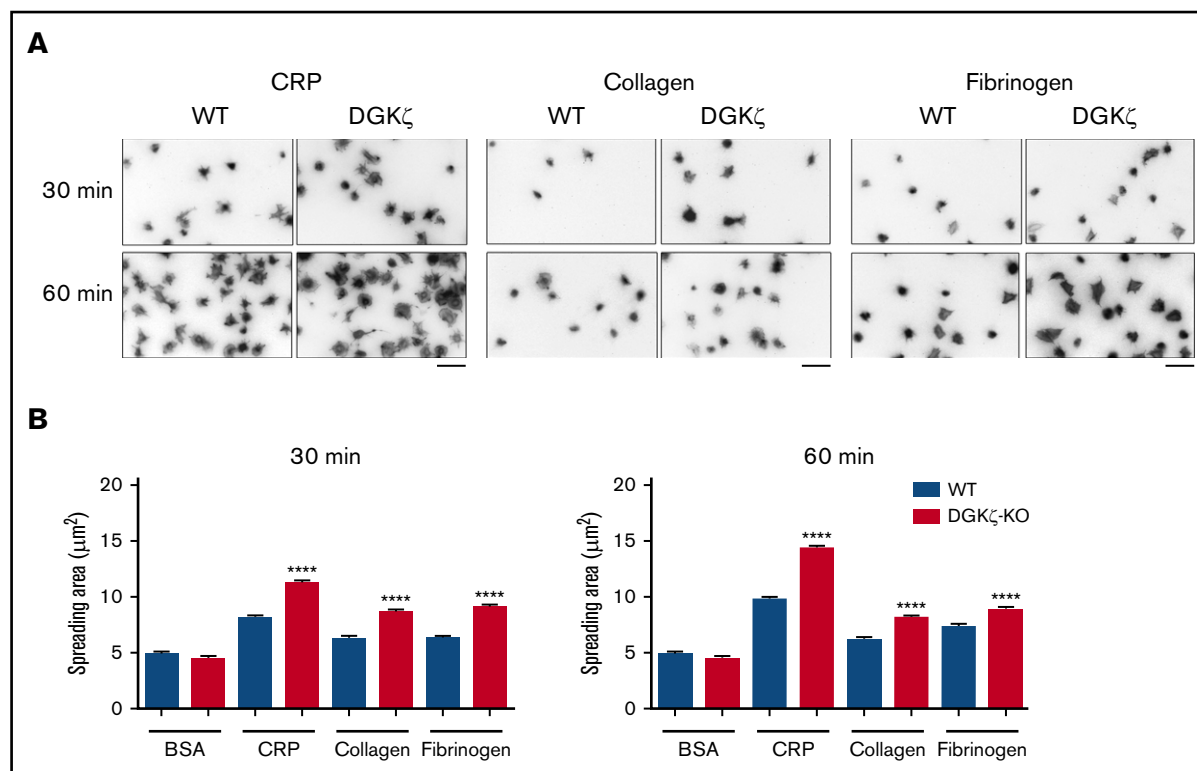


**Figure 2. DGK $\zeta$ -KO platelets exhibit enhanced platelet spreading on substrates for both GPVI and integrin  $\alpha$ IIb $\beta$ 3.** Washed platelets from WT and DGK $\zeta$ -KO mice were allowed to adhere on immobilized CRP (50  $\mu$ g/mL), collagen (50  $\mu$ g/mL), or fibrinogen (30  $\mu$ g/mL) for the indicated times at 37°C. After washing with phosphate-buffered saline to remove unbound platelets, adherent platelets were fixed and stained with phalloidin-TRITC. (A) Images of spread platelets representative of 3 independent experiments are shown. Bars represent 10  $\mu$ m. (B) The average area covered by individual platelets was quantified from at least 4 images per substrate and 250 to 500 platelets per time point. Spreading area is reported as the mean  $\pm$  SEM. Statistical analysis was performed using the unpaired Student *t* test. \*\*\*\**P* < .0001 of DGK $\zeta$ -KO as compared with WT.

thrombin or the PAR4-activating peptide (AYPGKG-NH<sub>2</sub>; supplemental Figure 1B) was reduced in DGK $\zeta$ -KO relative to WT platelets. Responses to ADP and the thromboxane A<sub>2</sub> mimetic U46619 were unaffected by DGK $\zeta$  deficiency. Consistent with the aggregation results, P-selectin exposure, activation of integrin  $\alpha$ IIb $\beta$ 3 (Jon/A binding), and dense granule secretion assessed by adenosine triphosphate were elevated after CRP stimulation but reduced after thrombin stimulation and were the same after ADP or U46619 stimulation in DGK $\zeta$ -KO relative to WT platelets (Figure 1D-E; supplemental Figure 1C). Calcium mobilization after CRP stimulation was also enhanced in DGK $\zeta$ -KO platelets (supplemental Figure 1D). As reported in type I DGK inhibitor-treated human platelets, thrombin-mediated calcium mobilization was reduced in DGK $\zeta$ -KO platelets.

To determine whether other DGKs have an additive effect on platelet activation, we treated WT and DGK $\zeta$ -KO platelets with a type I DGK inhibitor. Treatment with the type I DGK inhibitor R59022 did not affect CRP- or thrombin-mediated platelet activation, suggesting that DGK $\zeta$  is a major isozyme regulating mouse platelet activation (supplemental Figure 1E). To determine whether the differential effect of DGK $\zeta$  disruption on GPVI- and PAR-mediated platelet activation is due to the differential role of DAG in these pathways, platelet aggregation in DAG-treated platelets was analyzed. DAG treatment potentiated both CRP- and thrombin-mediated platelet activation, suggesting that DAG is a positive regulator for both pathways (supplemental Figure 1F).

Consistent with the aggregation and secretion results, DGK $\zeta$ -KO platelets spread faster and to a greater extent on both collagen and CRP and, somewhat unexpectedly, on immobilized fibrinogen as well (Figure 2A-B). Spreading on either of these substrates is known to be enhanced by secreted ADP.<sup>3,27</sup> In the case of GPVI, ADP is released as a result of interactions between GPVI/FcR $\gamma$  chain and collagen. In  $\alpha$ IIb $\beta$ 3/fibrinogen interactions, it is released as a consequence of  $\alpha$ IIb $\beta$ 3-mediated outside-in signal amplification, which, like signaling through GPVI, utilizes immunoreceptor tyrosine-based activation motif-mediated activation of the Syk $\rightarrow$ PLC $\gamma$ 2 pathway that generates IP<sub>3</sub> and DAG.<sup>24,28</sup> Addition of ADP or thrombin to either WT or DGK $\zeta$ -KO platelets (supplemental Figure 2) normalized the spreading response, demonstrating that the enhanced spreading of DGK $\zeta$ -KO platelets is due to enhanced signal amplification.

### DGK $\zeta$ -KO mice exhibit faster time vessel occlusion after arterial injury

Given the opposing effects of DGK $\zeta$  deficiency on in vitro measures of GPVI- and thrombin-mediated platelet activation, we investigated the consequences of DGK $\zeta$  deficiency for hemostasis in vivo. Tail resection bleeding time is highly dependent on thrombin-mediated platelet activation,<sup>29,30</sup> and ROTEM analyses used to support decisions made before surgery or to monitor anticoagulant therapy are initiated by addition of tissue factor to drive thrombin-mediated platelet activation as well. As shown in Figure 3A, DGK $\zeta$ -KO and WT



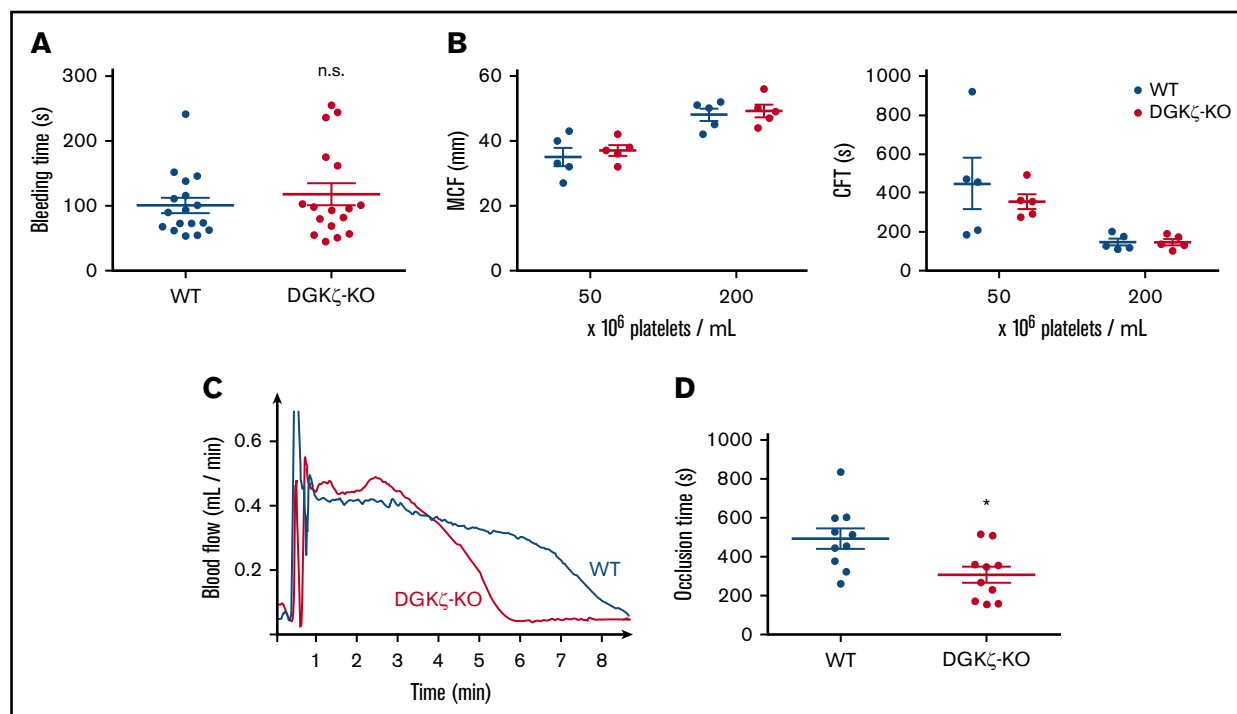


**Figure 3. DGK $\zeta$ -KO mice exhibit normal hemostasis but faster time to platelet plug formation after arterial injury.** (A) Bleeding assay was performed by tail tip amputation followed by immersion in phosphate-buffered saline at 37°C. Symbols represent times to cessation of bleeding for individual animals, and error bars represent the mean  $\pm$  SEM (n = 10-12). (B) ROTEM was performed using whole blood collected from WT and DGK $\zeta$ -KO mice and adjusted to the indicated platelet count. Results are shown as maximal clot firmness (MCF; n = 5; left) and clot formation time (CFT; n = 5; right). Symbols represent MCF and CFT for individual animals, and bars represent the mean  $\pm$  SEM. (C-D) The right carotid artery was injured by applying 10% FeCl $_3$  for 3 minutes. Blood flow was monitored with a Doppler flow probe until 3 minutes after full occlusion. (C) Representative flow traces for WT and DGK $\zeta$ -KO mice. (D) Symbols represent times to occlusion in individual animals, and bars represent the mean  $\pm$  SEM (n = 10). Statistical analysis was performed by the unpaired Student *t* test. \**P* < .05 of DGK $\zeta$ -KO as compared with WT.

mice had similar tail bleeding times, and blood from these mice showed no significant difference in ex vivo hemostatic plug formation in ROTEM chambers (Figure 3B), either under conditions of a normal platelet count ( $200 \times 10^6/\text{mL}$ ) or thrombocytopenia ( $50 \times 10^6/\text{mL}$ ). Taken together, these findings demonstrate that DGK $\zeta$  deficiency does not affect hemostasis initiated by thrombin. Notably, however, DGK $\zeta$  deficiency markedly improved time to vessel occlusion after FeCl $_3$ -induced carotid artery injury (Figure 3C-D), a GPVI-dependent event initiated by exposure of collagen at the site of injury.<sup>31,32</sup> Supplemental Figure 3 shows that the endothelial lining was disrupted and that collagen was exposed at the site of oxidative injury under the conditions employed in our FeCl $_3$  injury model. In vitro, DGK $\zeta$ -KO platelets adhered to a collagen-coated surface more rapidly and to a greater extent under arterial shear (Figure 4A-B), whereas the extent of thrombus growth after initial adhesion (a measure of thrombotic tendency) was not different from that of WT platelets (Figure 4C). These data are consistent with the platelet aggregation results (Figure 1) showing enhanced platelet reactivity to collagen.

### Increased GPVI expression in DGK $\zeta$ -KO platelets and megakaryocytes

To investigate the mechanism underlying enhanced GPVI-mediated platelet reactivity, we evaluated the effect of DGK $\zeta$  deficiency on platelet surface receptor expression. Interestingly, flow cytometric analysis revealed that the GPVI expression level on the platelet surface

was nearly 50% higher in DGK $\zeta$ -KO (mean fluorescence intensity, 3156) relative to WT platelets (mean fluorescence intensity, 2075), whereas surface expression of integrin  $\alpha 2$ , integrin  $\alpha \text{IIb}$ , PECAM-1, GPIIb $\alpha$ , and CLEC-2 was not affected (Figure 5A; supplemental Figure 4). Western blot analysis confirmed the increase in GPVI levels in DGK $\zeta$ -KO platelets, which interestingly did not have increased levels of the GPVI-associated Fc $\gamma$ R chain subunit (Figure 5B). These results indicate that DGK $\zeta$  deficiency specifically augments GPVI protein expression without affecting the expression of other receptors.

The level of protein expression in platelets and megakaryocytes is often, but not always, similar, including expression of GPVI.<sup>33-35</sup> To determine whether the increased level of platelet GPVI expression began during the megakaryocyte differentiation, we examined platelet surface receptor expression in mouse hematopoietic stem cell-derived megakaryocytes during differentiation. As shown in Figure 6A, surface GPVI was absent in both WT and DGK $\zeta$ -KO immature megakaryocytes and gradually increased during TPO-supported maturation. However, by day 5 of differentiation, GPVI expression was significantly higher in DGK $\zeta$ -KO megakaryocytes, suggesting that the enhanced GPVI expression that we saw in DGK $\zeta$ -KO platelets is attributable to upregulation of GPVI expression during megakaryocytopoiesis. In contrast, we did not see any difference in the level of expression of integrin  $\alpha 2$ , integrin  $\alpha \text{IIb}$ , or GPIIb $\alpha$  in DGK $\zeta$ -KO relative to WT megakaryocytes, consistent with that observed in DGK $\zeta$ -KO platelets (Figure 5). We further

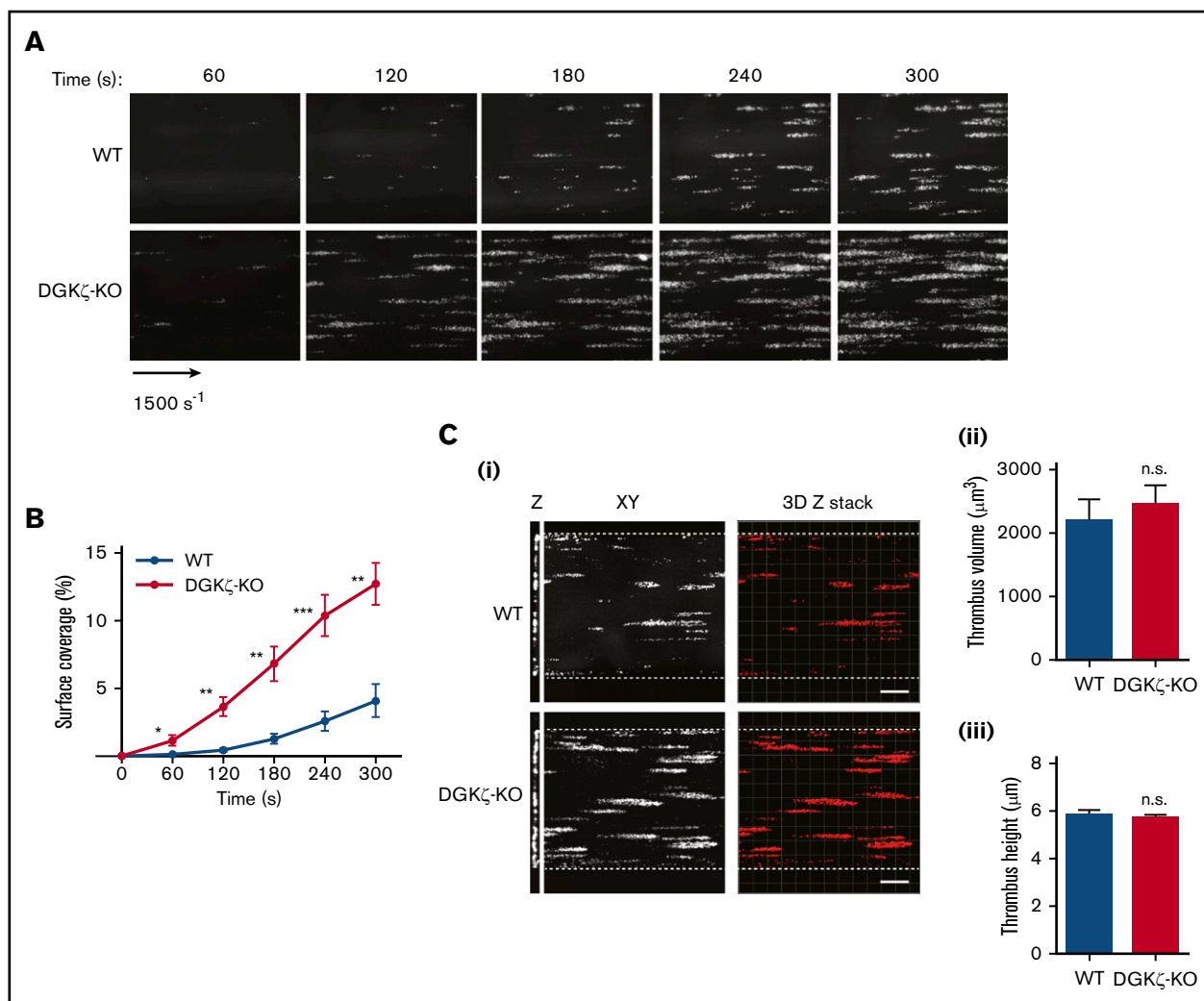


**Figure 4. DGK $\zeta$  deficiency improves platelet adhesion to collagen under conditions of flow.** Whole blood collected from WT and DGK $\zeta$ -KO mice was labeled with mepacrine and flowed over collagen-coated microchannels. (A) Representative images of platelet coverage under conditions of arterial shear ( $1500 \text{ s}^{-1}$ ). Images were taken under  $\times 20$  objective. (B) Surface area coverage at the indicated time points was quantified and reported as the mean  $\pm$  SEM ( $n = 6$ ). (C) Microchannels were washed after whole blood perfusion for 300 seconds and fixed, permeabilized, and stained with phalloidin-TRITC; Z stack images were then taken. (i) Representative Z stack images. Bars represent  $100 \mu\text{m}$ . The volume (ii) and height (iii) of each platelet thrombus at 300 seconds were quantified and reported as the mean  $\pm$  SEM ( $n = 5$ ; 76-116 thrombi per sample). Statistical analysis was performed by the unpaired Student  $t$  test. \* $P < .05$ , \*\* $P < .01$ , \*\*\* $P < .001$  of DGK $\zeta$ -KO as compared with WT.

investigated whether increased DAG in DGK $\zeta$ -KO platelets might be causing GPVI upregulation by adding DAG to the megakaryocyte culture. As shown in supplemental Figure 5, we did not see upregulation of GPVI by DAG treatment, suggesting that DGK $\zeta$  activity, rather than intracellular DAG, leads to GPVI upregulation. To examine whether GPVI expression is regulated at the transcriptional level in megakaryocytes, we determined the mRNA level of these receptors in mature megakaryocytes using quantitative PCR. In contrast to protein expression, GPVI mRNA levels did not differ significantly between WT and DGK $\zeta$ -KO megakaryocytes (Figure 6B), demonstrating that transcription of GPVI is comparable. There was also no difference in mRNA levels encoding the FcR $\gamma$  chain, integrin  $\alpha 2$ , integrin  $\alpha 1\text{b}$ , or GPIb $\alpha$ . These results suggest that protein expression of GPVI is regulated at the level of translation or that there is decreased GPVI degradation in DGK $\zeta$ -KO relative to WT megakaryocytes.

### Increased GPVI-mediated platelet signaling in DGK $\zeta$ -KO platelets

To examine the consequences of increased GPVI expression in DGK $\zeta$ -KO platelets, we investigated the activation state of signaling molecules downstream of GPVI stimulation. Previous studies in T cells have shown that DAG accumulates as a consequence of DGK $\zeta$  deficiency, resulting in increased ERK phosphorylation, a commonly used reporter of cytosolic DAG levels.<sup>21,22</sup> Consistent with the findings in T cells, both the rate and extent of ERK phosphorylation were significantly greater in DGK $\zeta$ -KO relative to WT platelets after addition of CRP (Figure 7A-B). Interestingly, activation of signaling molecules that are upstream of DAG generation in the GPVI signal transduction pathway, such as PLC $\gamma 2$  and Akt, was also increased in DGK $\zeta$ -KO platelets, suggesting that DGK $\zeta$  also influences early signaling events, perhaps as a result of the

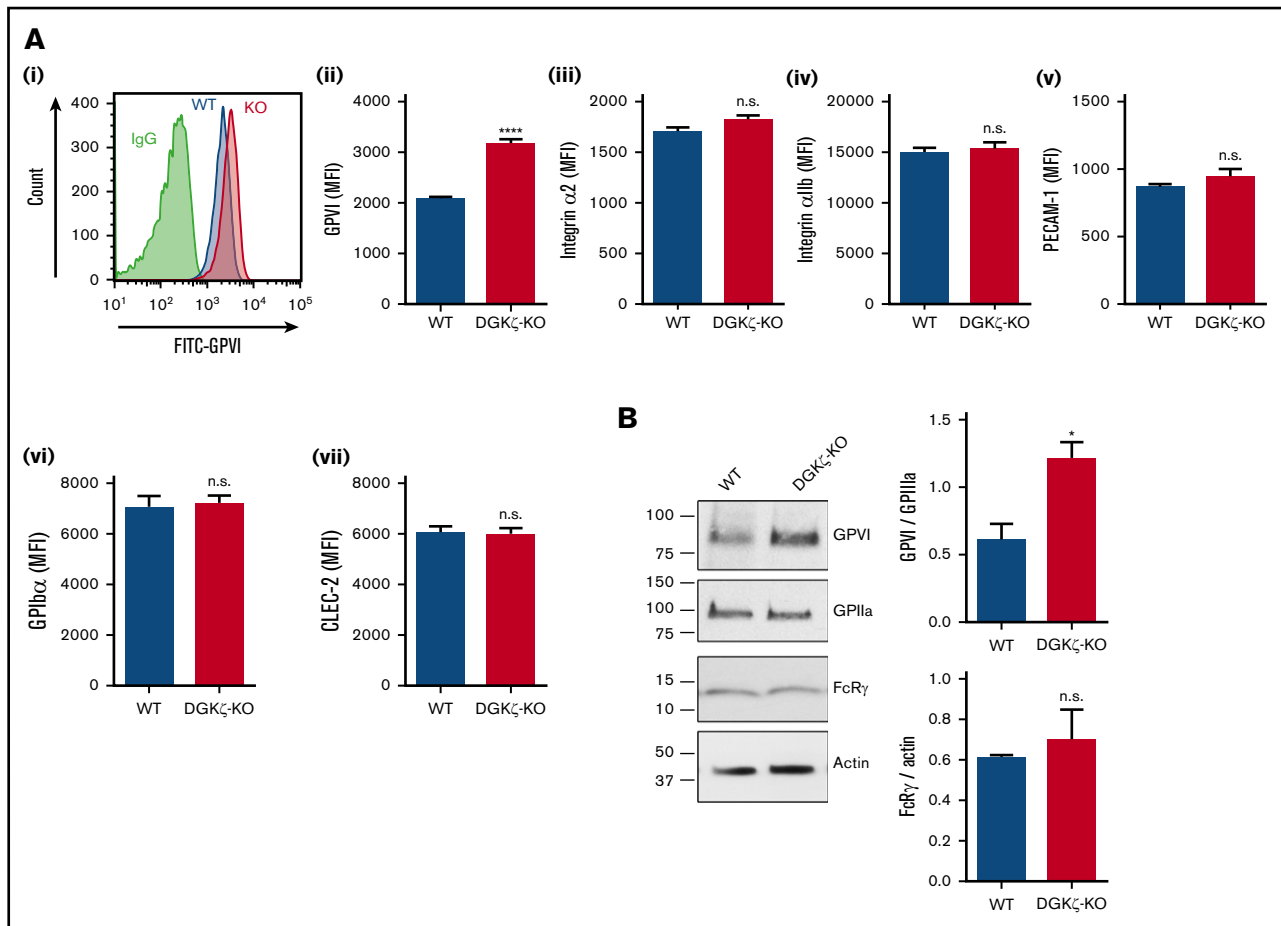


**Figure 5. Increased expression of GPVI in DGK $\zeta$ -KO platelets.** (A) Platelet surface receptor expression of GPVI (i-ii), integrin  $\alpha 2$  (iii), integrin  $\alpha IIb$  (iv), PECAM-1 (v), GPIIb $\alpha$  (vi), and CLEC-2 (vii) was measured in diluted whole blood samples from WT and DGK $\zeta$ -KO mice by flow cytometry. Mean fluorescence intensity (MFI) is reported as the mean  $\pm$  SEM ( $n = 10$ ). (B) Whole lysates of washed platelets from WT and DGK $\zeta$ -KO mice were analyzed by western blotting for GPVI, GPIIIa, FcR $\gamma$  chain, and actin. The blots are representative of 4 independent experiments. Quantification of band densities (right) is reported as the mean  $\pm$  SEM ( $n = 4$ ). Statistical analysis was performed using the unpaired Student  $t$  test. \* $P < .05$ , \*\*\*\* $P < .0001$  of DGK $\zeta$ -KO as compared with WT platelets. FITC, fluorescein isothiocyanate; IgG, immunoglobulin G.

increased static level of GPVI on the platelet surface. Phosphorylation of the negative regulatory tyrosine (Tyr 507) on the Src family kinase Lyn was also found to be significantly reduced in DGK $\zeta$ -KO platelets, even under resting conditions, suggesting that Lyn is in more primed state. Taken together, these data demonstrate that DGK $\zeta$  deficiency results in increased surface expression of GPVI and that increased expression of this adhesion and signaling receptor produces platelets that are in a potentiated, more easily activatable state.

## Discussion

DAG is an important secondary messenger that regulates platelet activation. Cytosolic levels of DAG are regulated by DGKs, which phosphorylate DAG, thereby lowering its concentration. Although the roles of DGKs in T-cell responsiveness have been well studied, DGK roles in platelet activation have not been fully examined. In the present study, we show that a specific DGK isoform, DGK $\zeta$ , is expressed in platelets and megakaryocytes and that it negatively regulates GPVI-mediated platelet reactivity in mice. Although it is

unclear whether DGK $\zeta$  in other cell types affects hemostasis, we found that platelets from DGK $\zeta$ -KO mice have enhanced responsiveness to GPVI-specific agonists and that DGK $\zeta$  deficiency leads to upregulation of GPVI surface expression. This is the first study demonstrating a role for DGK $\zeta$  in platelet activation.

To date, only pharmacological inhibitors have been used to examine the function of DGKs in human platelets. Although these inhibitors preferentially target type I DGKs ( $\alpha$ ,  $\beta$ , and  $\gamma$ ) and have little or no effect on DGK $\zeta$  activity,<sup>36</sup> they have nevertheless shown that type I DGKs have a negative regulatory role in GPVI-mediated platelet activation and contradictory roles in regulating thrombin-mediated platelet activation, with some studies showing enhancement and others showing suppression of platelet aggregation and Ca<sup>2+</sup> influx.<sup>10-12</sup> These opposing results could be due to off-target effects of the inhibitors or the concentration of the agonists and inhibitors used.

Our results using DGK $\zeta$ -KO mice, platelets, and megakaryocytes demonstrate that DGK $\zeta$  functions to negatively regulate GPVI-mediated platelet activation, while having a mild but positive



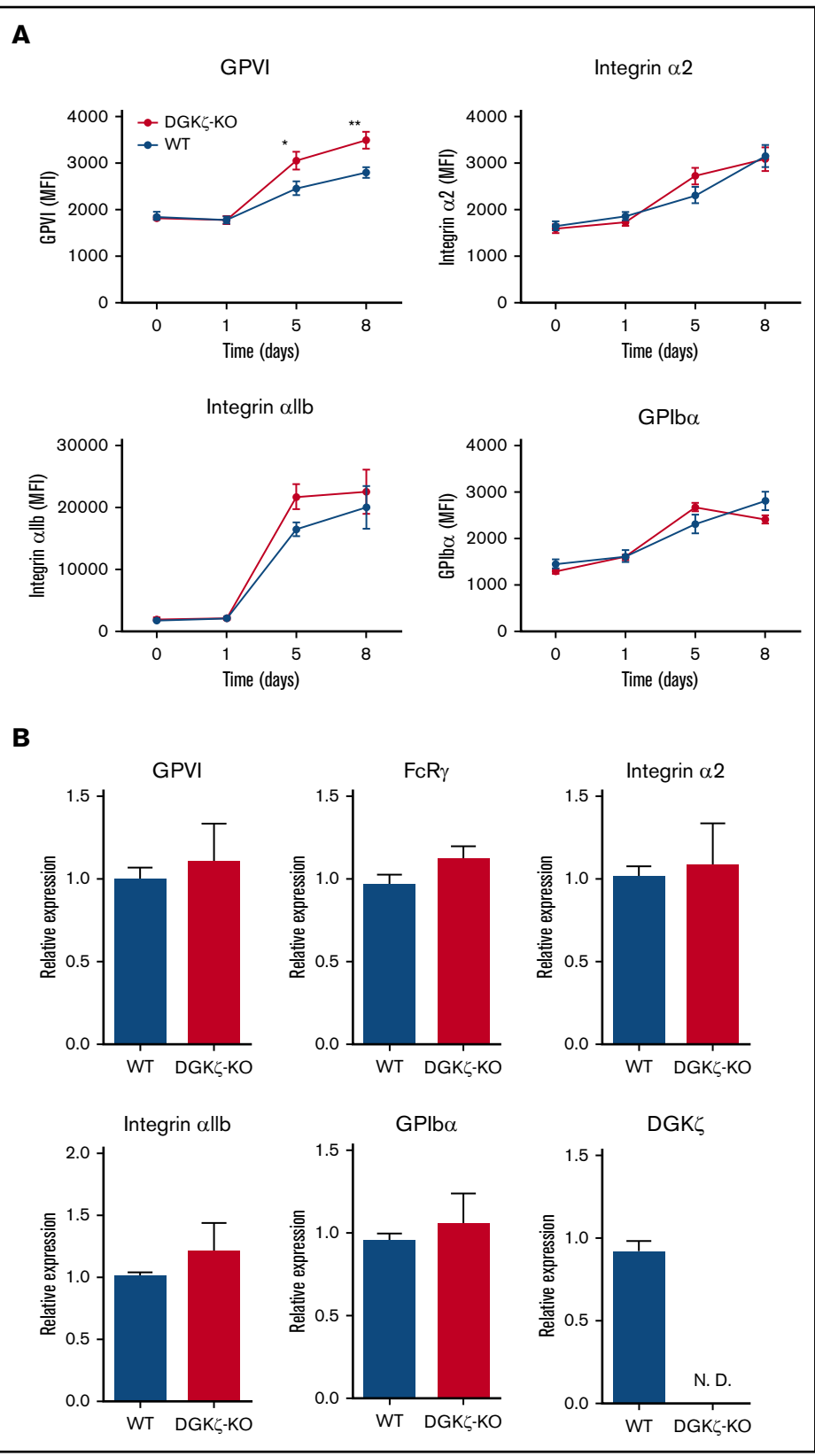


**Figure 6. DGK $\zeta$  deficiency enhances surface expression of GPVI without increased messenger RNA (mRNA) in murine megakaryocytes.** (A) Bone marrow–derived hematopoietic stem cells from WT and DGK $\zeta$ -KO mice were cultured in TPO plus SCF for 0, 1, 5, or 8 days to obtain megakaryocytes, and surface expression of GPVI, integrin  $\alpha$ 2, integrin  $\alpha$ IIb, and GPIb $\alpha$  was measured by flow cytometry. Mean fluorescence intensity (MFI) is reported as the mean  $\pm$  SEM (n = 6). (B) Mature megakaryocytes were enriched by using a BSA density gradient, and RNA was extracted. Quantitative RT-PCR was performed, and relative expression levels of GPVI, FcR $\gamma$  chain, integrin  $\alpha$ 2, integrin  $\alpha$ IIb, GPIb $\alpha$ , and DGK $\zeta$  in DGK $\zeta$ -KO megakaryocytes are shown relative to WT expression levels (n = 5). Hypoxanthine-guanine phosphoribosyltransferase was used for normalization. \* $P$  < .05, \*\* $P$  < .01 of DGK $\zeta$ -KO as compared with WT megakaryocytes. N.D., not detectable.

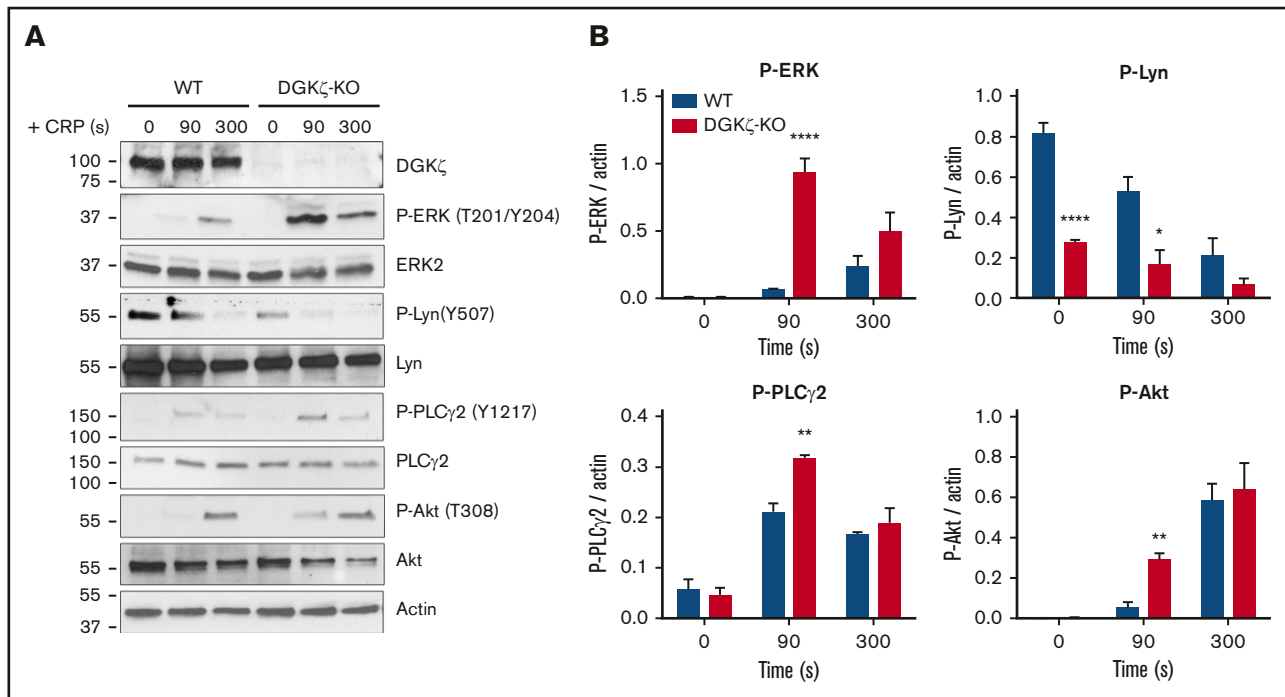


**Figure 7. DGK $\zeta$  deficiency enhances signaling in response to GPVI activation.** WT and DGK $\zeta$ -KO washed platelets were stimulated with 1  $\mu$ g/mL of CRP for 90 and 300 seconds under stirring conditions in an aggregometer. Lysates were analyzed for DGK $\zeta$ , phosphorylated ERK (P-ERK; Thr202/Tyr204), ERK2, P-Lyn (Tyr 507), Lyn, P-PLC $\gamma$ 2 (Tyr 1217), PLC $\gamma$ 2, P-Akt (Thr 308), Akt, and actin. (A) Blot shown is representative of 3 independent experiments. (B) Quantification of band densities normalized to actin over all experiments is reported as the mean  $\pm$  SEM (n = 3). Statistical analysis was performed using the unpaired Student *t* test. \**P* < .05, \*\**P* < .01, \*\*\*\**P* < .0001 of DGK $\zeta$ -KO as compared with WT platelets.

regulating influence on platelet activation induced by low-dose thrombin. The enhanced responsiveness to GPVI-specific agonists in DGK $\zeta$ -KO platelets is mediated by 2 pathways, shown in supplemental Figure 6. The first is through upregulating the cell surface expression levels of GPVI, leading to enhanced activation of signaling molecules immediately downstream of this receptor, including Lyn and PLC $\gamma$ 2, and the other is through enhanced Ras-ERK signaling, an often-used sensitive reporter of intracellular DAG levels and enhanced PKC activation. Currently, we cannot separate the relative importance of the 2 pathways in the enhanced responsiveness of DGK $\zeta$ -KO platelets, because DGK $\zeta$ -specific inhibitors have not yet been developed. Their availability would enable us to determine whether short-term DGK $\zeta$  inhibition, as opposed to genetic deletion from birth, can increase cell surface expression of GPVI and/or the activation of ERK signaling in mouse and human platelets.

Similar to previous studies using pharmacological inhibition by type I DGK inhibitors, we observed (Figure 1) that genetic deletion of DGK $\zeta$  results in enhanced platelet aggregation to collagen and CRP, while at the same time conferring a somewhat reduced response to low-dose, but not high-dose, thrombin. These findings are consistent with the observation that tail vein bleeding times and ROTEM analysis, both initiated by relatively high doses of thrombin, are largely the same in WT and DGK $\zeta$ -KO mice (Figure 3), whereas vessel occlusion time after FeCl $_3$  vessel injury, which is thought to expose subendothelial collagen fibers, is more rapid in DGK $\zeta$ -KO mice. Interestingly, mice in which the DGK $\epsilon$  isozyme has been knocked down exhibit a prothrombotic

phenotype, including enhanced platelet adhesion to endothelial cells *in vitro*,<sup>37</sup> consistent with our observations of more rapid occlusion in DGK $\zeta$ -KO mice.

Nevertheless, it remains unclear how DGK $\zeta$  differentially regulates GPVI- vs thrombin-mediated platelet responsiveness. One speculation is that GPVI and thrombin use different subtypes of PLC, with GPVI using PLC $\gamma$ 2 and thrombin using PLC $\beta$ , because the subcellular location and access to substrates could affect the DGK $\zeta$  activity. A similar phenotype has been reported for PKC $\delta$ , which limits secretion and aggregation in GPVI-mediated platelet activation but enhances them under thrombin stimulation,<sup>38-40</sup> suggesting PKC activation could be differentially regulated under these pathways. Another possibility is that depletion of DGK $\zeta$  reduces the available pool of PA, leading to reduced platelet responsiveness. The role of PA in enhancing thrombin-mediated platelet activation has been suggested by Marumo et al,<sup>10</sup> who reported that treatment of human platelets with propranolol, an inhibitor of PA phosphatase, enhanced Ca $^{2+}$  entry after thrombin stimulation.

One of the fascinating observations in the present study was the finding that DGK $\zeta$ -KO platelets have increased expression of GPVI without affecting the total cellular expression of its noncovalently-linked partner, the FcR $\gamma$  chain. This is consistent with reports showing that even though FcR $\gamma$  chain-deficient platelets do not express GPVI,<sup>41</sup> GPVI-deficient platelets have normal FcR $\gamma$  chain expression,<sup>42</sup> which is perhaps coupled with other adhesion receptors like GPIb as well.<sup>43</sup> These results suggest that the FcR $\gamma$  chain is expressed in excess of that required to traffic GPVI to the cell surface.

The biochemical explanation for increased GPVI expression remains to be explored and could theoretically involve transcriptional, post-translational, and/or cellular trafficking and degradation levels of control. Studies in other cell types have shown that DGK $\zeta$  mainly localizes in the nucleus in neurons and lung cells and actually associates with chromatin,<sup>44</sup> suggesting that DGK $\zeta$  can directly or indirectly regulate transcription. However, because DGK $\zeta$ -KO megakaryocytes have increased GPVI levels without any difference in their mRNA levels (Figure 6), it is unlikely that DGK $\zeta$  regulates GPVI transcription. It is also possible that surface expression levels of GPVI could be regulated by metalloproteinase-mediated shedding; however, because shedding is known to occur upon cellular activation,<sup>45</sup> and GPVI levels are already constitutively upregulated in both resting DGK $\zeta$ -KO platelets and megakaryocytes, shedding is unlikely the mechanism underlying the increased GPVI expression levels in DGK $\zeta$ -KO cells. Preliminary studies in our laboratory using proteasome inhibitors suggest that DGK $\zeta$  deficiency might be causing reduced GPVI degradation. Examining the cell and molecular regulation of GPVI expression levels in megakaryocytes and platelets will thus require further investigation.

Finally, there seems to be growing interest in the pathophysiology of DGKs in human health and disease. Loss-of-function mutations in DGK $\epsilon$  have recently been implicated in atypical hemolytic-uremic syndrome,<sup>46</sup> perhaps because of a hyperactive renal endothelium that predisposed the patient to localized thrombosis, leading to renal failure. In the field of cancer, Riese et al<sup>47</sup> recently proposed that development of novel inhibitors targeting the  $\alpha$  and  $\zeta$  isoforms of DGK could be useful in improving the reactivity of tumor-specific T cells that are increasingly being employed in immunotherapy. The finding in the present work that such reagents also have the

potential to augment platelet reactivity suggests that caution must be exerted before widespread adoption of this strategy. Additional work is thus warranted to identify the cell-type specificity and action of DGKs in thrombosis, hemostasis, vascular biology, and immunology.

## Acknowledgments

The authors thank the members of the Yan-Qing Ma laboratory at the Blood Research Institute for help in setting up the ferric chloride arterial injury model.

This work was supported by National Institutes of Health, National Heart, Lung, and Blood Institute grants R01 HL-130054 and R35 HL-139937 (P.J.N.) and by a T32 training grant from the National Heart, Lung, and Blood Institute of the National Institutes of Health (A.J.M.).

## Authorship

Contribution: A.J.M. designed and performed experiments, analyzed data, created the figures, and wrote the manuscript; N.M.Z. designed and performed experiments and analyzed data; M.J.R. provided important material; D.K.N. designed experiments and wrote the manuscript; and P.J.N. designed experiments, wrote the manuscript, and supervised the work.

Conflict-of-interest disclosure: The authors declare no competing financial interests.

Correspondence: Peter J. Newman, Blood Research Institute, Versiti, PO Box 21 78, Milwaukee, WI 53201; e-mail: peter.newman@bcw.edu.

## References

1. Savage B, Saldivar E, Ruggeri ZM. Initiation of platelet adhesion by arrest onto fibrinogen or translocation on von Willebrand factor. *Cell*. 1996;84(2):289-297.
2. Werner MH, Bielawska AE, Hannun YA. Quantitative analysis of diacylglycerol second messengers in human platelets: correlation with aggregation and secretion. *Mol Pharmacol*. 1992;41(2):382-386.
3. Li Z, Delaney MK, O'Brien KA, Du X. Signaling during platelet adhesion and activation. *Arterioscler Thromb Vasc Biol*. 2010;30(12):2341-2349.
4. Carman GM, Han GS. Phosphatidic acid phosphatase, a key enzyme in the regulation of lipid synthesis. *J Biol Chem*. 2009;284(5):2593-2597.
5. Estevez B, Du X. New concepts and mechanisms of platelet activation signaling. *Physiology (Bethesda)*. 2017;32(2):162-177.
6. Topham MK. Signaling roles of diacylglycerol kinases. *J Cell Biochem*. 2006;97(3):474-484.
7. Joshi RP, Koretzky GA. Diacylglycerol kinases: regulated controllers of T cell activation, function, and development. *Int J Mol Sci*. 2013;14(4):6649-6673.
8. van Blitterswijk WJ, Houssa B. Properties and functions of diacylglycerol kinases. *Cell Signal*. 2000;12(9-10):595-605.
9. Yada Y, Ozeki T, Kanoh H, Nozawa Y. Purification and characterization of cytosolic diacylglycerol kinases of human platelets. *J Biol Chem*. 1990;265(31):19237-19243.
10. Marumo M, Nakano T, Takeda Y, Goto K, Wakabayashi I. Inhibition of thrombin-induced Ca<sup>2+</sup> influx in platelets by R59949, an inhibitor of diacylglycerol kinase. *J Pharm Pharmacol*. 2012;64(6):855-861.
11. de Chaffoy de Courcelles D, Roevens P, Van Belle H, Kennis L, Somers Y, De Clerck F. The role of endogenously formed diacylglycerol in the propagation and termination of platelet activation. A biochemical and functional analysis using the novel diacylglycerol kinase inhibitor, R 59 949. *J Biol Chem*. 1989;264(6):3274-3285.
12. Guidetti GF, Lova P, Bernardi B, et al. The Gi-coupled P2Y12 receptor regulates diacylglycerol-mediated signaling in human platelets. *J Biol Chem*. 2008;283(43):28795-28805.
13. Joseph S, Krishnamurthi S, Kakkar VV. Differential effects of the diacylglycerol kinase inhibitor R59022 on thrombin versus collagen-induced human platelet secretion. *Biochim Biophys Acta*. 1988;969(1):9-17.

14. Nunn DL, Watson SP. A diacylglycerol kinase inhibitor, R59022, potentiates secretion by and aggregation of thrombin-stimulated human platelets. *Biochem J*. 1987;243(3):809-813.
15. Goto K, Kondo H. A 104-kDa diacylglycerol kinase containing ankyrin-like repeats localizes in the cell nucleus. *Proc Natl Acad Sci USA*. 1996;93(20):11196-11201.
16. Bunting M, Tang W, Zimmerman GA, McIntyre TM, Prescott SM. Molecular cloning and characterization of a novel human diacylglycerol kinase zeta. *J Biol Chem*. 1996;271(17):10230-10236.
17. Goto K, Kondo H. Diacylglycerol kinase in the central nervous system--molecular heterogeneity and gene expression. *Chem Phys Lipids*. 1999;98(1-2):109-117.
18. Ding L, McIntyre TM, Zimmerman GA, Prescott SM. The cloning and developmental regulation of murine diacylglycerol kinase zeta. *FEBS Lett*. 1998;429(1):109-114.
19. Zhong XP, Hainey EA, Olenchock BA, et al. Enhanced T cell responses due to diacylglycerol kinase zeta deficiency. *Nat Immunol*. 2003;4(9):882-890.
20. Joshi RP, Schmidt AM, Das J, et al. The  $\zeta$  isoform of diacylglycerol kinase plays a predominant role in regulatory T cell development and TCR-mediated ras signaling. *Sci Signal*. 2013;6(303):ra102.
21. Zhong XP, Hainey EA, Olenchock BA, Zhao H, Topham MK, Koretzky GA. Regulation of T cell receptor-induced activation of the Ras-ERK pathway by diacylglycerol kinase zeta. *J Biol Chem*. 2002;277(34):31089-31098.
22. Riese MJ, Wang LC, Moon EK, et al. Enhanced effector responses in activated CD8+ T cells deficient in diacylglycerol kinases. *Cancer Res*. 2013;73(12):3566-3577.
23. Rowley JW, Oler AJ, Tolley ND, et al. Genome-wide RNA-seq analysis of human and mouse platelet transcriptomes. *Blood*. 2011;118(14):e101-e111.
24. Zhi H, Rauova L, Hayes V, et al. Cooperative integrin/ITAM signaling in platelets enhances thrombus formation in vitro and in vivo. *Blood*. 2013;121(10):1858-1867.
25. Bercovitz RS, Brenner MK, Newman DK. A whole blood model of thrombocytopenia that controls platelet count and hematocrit. *Ann Hematol*. 2016;95(11):1887-1894.
26. Liu CH, Machado FS, Guo R, et al. Diacylglycerol kinase zeta regulates microbial recognition and host resistance to *Toxoplasma gondii*. *J Exp Med*. 2007;204(4):781-792.
27. O'Brien KA, Gartner TK, Hay N, Du X. ADP-stimulated activation of Akt during integrin outside-in signaling promotes platelet spreading by inhibiting glycogen synthase kinase-3 $\beta$ . *Arterioscler Thromb Vasc Biol*. 2012;32(9):2232-2240.
28. Boylan B, Gao C, Rathore V, Gill JC, Newman DK, Newman PJ. Identification of Fc $\gamma$ RIIa as the ITAM-bearing receptor mediating  $\alpha$ IIb $\beta$ 3 outside-in integrin signaling in human platelets. *Blood*. 2008;112(7):2780-2786.
29. Sambrano GR, Weiss EJ, Zheng YW, Huang W, Coughlin SR. Role of thrombin signalling in platelets in haemostasis and thrombosis. *Nature*. 2001;413(6851):74-78.
30. Bynagari-Settipalli YS, Cornelissen I, Palmer D, et al. Redundancy and interaction of thrombin- and collagen-mediated platelet activation in tail bleeding and carotid thrombosis in mice. *Arterioscler Thromb Vasc Biol*. 2014;34(12):2563-2569.
31. Dubois C, Panicot-Dubois L, Merrill-Skoloff G, Furie B, Furie BC. Glycoprotein VI-dependent and -independent pathways of thrombus formation in vivo. *Blood*. 2006;107(10):3902-3906.
32. Furie B, Furie BC. Thrombus formation in vivo. *J Clin Invest*. 2005;115(12):3355-3362.
33. Machlus KR, Italiano JE Jr. The incredible journey: from megakaryocyte development to platelet formation. *J Cell Biol*. 2013;201(6):785-796.
34. Lagrue-Lak-Hal AH, Debili N, Kingbury G, et al. Expression and function of the collagen receptor GPVI during megakaryocyte maturation. *J Biol Chem*. 2001;276(18):15316-15325.
35. Smith CW, Thomas SG, Raslan Z, et al. Mice lacking the inhibitory collagen receptor LAIR-1 exhibit a mild thrombocytosis and hyperactive platelets. *Arterioscler Thromb Vasc Biol*. 2017;37(5):823-835.
36. Jiang Y, Sakane F, Kanoh H, Walsh JP. Selectivity of the diacylglycerol kinase inhibitor 3-[2-(4-[bis-(4-fluorophenyl)methylene]-1-piperidinyl)ethyl]-2,3-dihydro-2-thioxo-4(1H)quinazolinone (R59949) among diacylglycerol kinase subtypes. *Biochem Pharmacol*. 2000;59(7):763-772.
37. Bruneau S, Néel M, Roumenina LT, et al. Loss of DGK $\epsilon$  induces endothelial cell activation and death independently of complement activation. *Blood*. 2015;125(6):1038-1046.
38. Zaid Y, Senhaji N, Darif Y, Kojok K, Oudghiri M, Naya A. Distinctive roles of PKC delta isozyme in platelet function. *Curr Res Transl Med*. 2016;64(3):135-139.
39. Chari R, Kim S, Murugappan S, Sanjay A, Daniel JL, Kunapuli SP. Lyn, PKC-delta, SHIP-1 interactions regulate GPVI-mediated platelet-dense granule secretion. *Blood*. 2009;114(14):3056-3063.
40. Bhavanasri D, Kostyak JC, Swindle J, Kilpatrick LE, Kunapuli SP. CGX1037 is a novel PKC isoform delta selective inhibitor in platelets. *Platelets*. 2015;26(1):2-9.
41. Nieswandt B, Bergmeier W, Schulte V, Rackebrandt K, Gessner JE, Zirngibl H. Expression and function of the mouse collagen receptor glycoprotein VI is strictly dependent on its association with the Fc $\gamma$  chain. *J Biol Chem*. 2000;275(31):23998-24002.
42. Kato K, Kanaji T, Russell S, et al. The contribution of glycoprotein VI to stable platelet adhesion and thrombus formation illustrated by targeted gene deletion. *Blood*. 2003;102(5):1701-1707.

43. Falati S, Edmead CE, Poole AW. Glycoprotein Ib-V-IX, a receptor for von Willebrand factor, couples physically and functionally to the Fc receptor gamma-chain, Fyn, and Lyn to activate human platelets. *Blood*. 1999;94(5):1648-1656.
44. Hasegawa H, Nakano T, Hozumi Y, et al. Diacylglycerol kinase zeta is associated with chromatin, but dissociates from condensed chromatin during mitotic phase in NIH3T3 cells. *J Cell Biochem*. 2008;105(3):756-765.
45. Gardiner EE, Karunakaran D, Shen Y, Arthur JF, Andrews RK, Berndt MC. Controlled shedding of platelet glycoprotein (GP)VI and GPIb-IX-V by ADAM family metalloproteinases. *J Thromb Haemost*. 2007;5(7):1530-1537.
46. Lemaire M, Frémeaux-Bacchi V, Schaefer F, et al. Recessive mutations in DGKE cause atypical hemolytic-uremic syndrome. *Nat Genet*. 2013;45(5):531-536.
47. Riese MJ, Moon EK, Johnson BD, Albelda SM. Diacylglycerol kinases (DGKs): novel targets for improving T cell activity in cancer. *Front Cell Dev Biol*. 2016;4:108.